Tissue-Tek). To measure plaque size, longitudinal sections (about 30 per mouse) of the aortic arch were analysed microscopically for all mice. For this purpose, a 3-mm segment of the lesser curvature of the aortic arch was defined proximally by a perpendicular axis dropped from the right side of the innominate artery origin (Fig. 6, dashed line) and the aortic-arch wall area subtended by this 3-mm stretch of intima was calculated for each section of all mice by computerized image analysis (Fig. 6, green line). The aortic-arch wall thickness was determined on this same segment of the lesser curvature (Fig. 6, red line). The maximal area and thickness of the inner-aortic-arch wall of each mouse were used to compute averages per group.

For immunofluorescence double-staining, cryostat sections (5 μm) of the aortic arch were cut, air-dried, fixed in acetone, and stained with anti-CD40L, anti-CD40, or anti-VCAM-1 antibodies (PharMingen), or with the respective cell-specific antibody (anti-CD31 for endothelial cells, anti-α actin for smooth-muscle cells, anti-MAC3 for macrophages, and anti-CD3 for T lymphocytes; Dako) as described[5]. Areas that stained positive for macrophages were measured using computer-assisted image quantification (Optimas 5.2, Optimas Corporation). Lymphocytes identified by anti-CD3 staining were counted microscopically by two blinded observers. Controls for specificity included staining with the species-respective immunoglobulin (mouse myeloma protein MOPC-21, Sigma; rat and rabbit immunoglobulin, Dako). The abdominal aortas were fixed with 10% buffered formalin and stained for lipid deposition with Sudan IV (Fisher Scientific). The aortas were then opened longitudinally to the iliac bifurcation and pinned out on black wax surface using 0.2-mm steel pins. The percentage of stain deposition was calculated within the total surface area (15 mm from the iliac bifurcation to the thoracic section of the aorta) using computer analysis[26,27].

Received 9 February; accepted 27 April 1998.

1. Ross, R. The pathogenesis of atherosclerosis: a perspective for the 1990s. *Nature* **362,** 801–809 (1993).
2. Fuster, V., Lewis, A. Conner Memorial Lecture. Mechanisms leading to myocardial infarction: insights from studies of vascular biology. *Circulation* **90,** 2126–2146 (1996).
3. Fuster, V., Badimon, L., Badimon, J. J. & Chesebro, J. H. The pathogenesis of coronary artery disease and the acute coronary syndromes. *N. Engl. J. Med.* **326,** 242–250 (1992).
4. Hansson, G. K. *et al.* Localization of T lymphocytes and macrophages in fibrous and complicated human atherosclerotic plaques. *Arteriosclerosis* **72,** 135–141 (1988).
5. Mach, F. *et al.* Functional CD40 ligand is expressed on human vascular endothelial cells, smooth muscle cells, and macrophages: implications for CD40-CD40 ligand signaling in atherosclerosis. *Proc. Natl Acad. Sci. USA* **94,** 1931–1936 (1997).
6. Foy, T. M., Aruffo, A., Bajorath, J., Buhlmann, J. E. & Noelle, R. J. Immune regulation by CD40 and its ligand gp39. *Annu. Rev. Immunol.* **14,** 591–617 (1996).
7. Zhou, X., Stemme, S. & Hansson, G. K. Evidence for a local immune response in atherosclerosis. *Am. J. Pathol.* **149,** 359–366 (1996).
8. Lichtman, A. H., Cybulsky, M. & Luscinskas, F. W. Immunology of atherosclerosis: the promise of mouse models. *Am. J. Pathol.* **149,** 351–357 (1996).
9. Emeson, E. E. & Robertson, A. L. Jr T lymphocytes in aortic and coronary intimas. Their potential role in atherogenesis. *Am. J. Pathol.* **130,** 369–375 (1988).
10. Durie, F. H. *et al.* Prevention of collagen-induced arthritis with an antibody to gp39, the ligand for CD40. *Science* **261,** 1328–1330 (1993).
11. Mohan, C., Shi, Y., Laman, J. D. & Datta, S. K. Interaction between CD40 and its ligand gp39 in the development of murine lupus nephritis. *J. Immunol.* **154,** 1470–1480 (1995).
12. Larsen, C. P. *et al.* Long-term acceptance of skin and cardiac allografts after blocking CD40 and CD28 pathways. *Nature* **381,** 434–438 (1996).
13. Gerritse, K. *et al.* CD40-CD40 ligand interactions in experimental allergic encephalomyelitis and multiple sclerosis. *Proc. Natl Acad. Sci. USA* **93,** 2499–2504 (1996).
14. Carayanniotis, G., Master, S. R. & Noelle, R. J. Suppression of murine thyroiditis via blockade of the CD40-CD40L interaction. *Immunity* **90,** 421–426 (1997).
15. Schönbeck, U. *et al.* Regulation of matrix metalloproteinase expression in human vascular smooth muscle cells by T lymphocytes: a role for CD40 signaling in plaque rupture? *Circ. Res.* **81,** 448–454 (1997).
16. Mach, F., Schönbeck, U., Bonnefoy, J.-Y., Pober, J. S. & Libby, P. Activation of monocyte/macrophage functions related to acute atheroma complication by ligation of CD40. Induction of collagenase, stromelysin, and tissue factor. *Circulation* **96,** 396–399 (1997).
17. Karmann, K., Hughes, C. C. W., Schechner, J., Fanslow, W. C. & Pober, J. S. CD40 on human endothelial cells: inducibility by cytokines and functional regulation of adhesion molecule expression. *Proc. Natl Acad. Sci. USA* **92,** 4342–4346 (1995).
18. Yellin, M. J. *et al.* Functional interaction of T cells with endothelial cells: the role of D40L-CD40-mediated signals. *J. Exp. Med.* **182,** 1857–1864 (1995).
19. Hollenbaugh, D. *et al.* Expression of functional CD40 by vascular endothelial cells. *J. Exp. Med.* **182,** 33–40 (1995).
20. Mach, F., Schönbeck, U. & Libby, P. CD40 signaling in vascular cells: a key role in atherosclerosis? *Atherosclerosis* (in the press).
21. Ishibashi, S. *et al.* Hypercholesterolemia in low density lipoprotein receptor knockout mice and its reversal by adenovirus-mediated gene delivery. *J. Clin. Invest.* **92,** 883–893 (1993).
22. Lichtman, A. H. *et al.* Comparative effects of precisely defined semipurified diets supplemented with lipid, cholesterol, and sodium cholate on serum-lipids and aortic atherosclerosis LDL. *FASEB J.* **11,** A154 (1997).
23. Kennedy, M. K. *et al.* CD40/CD40 ligand interactions are required for T cell-dependent production of interleukin-12 by mouse macrophages. *Eur. J. Immunol.* **26,** 370–378 (1996).
24. Lu, L. *et al.* Blockade of the CD40-CD40L pathway potentiates the capacity of donor-derived dendritic cell progenitors to induce long-term cardiac allograft survival. *Transplantation* **64,** 1808–1815 (1997).
25. Yokode, Y., Hammer, R. E., Ishibashi, S., Brown, M. S. & Goldstein, J. L. Diet-induced hypercholesterolemia in mice: prevention by overexpression of LDL receptors. *Science* **250,** 1273–1275 (1990).
26. Johnson, R. C. *et al.* Absence of P-selectin delays fatty streak formation in mice. *J. Clin. Invest.* **99,** 1037–1043 (1997).
27. Tangirals, R. K., Rubin, E. M. & Palinski, W. Quantitation of atherosclerosis in murine models: correlation between lesions in the aortic origin and in the entire aorta, and differences in the extent of lesions between sexes in LDL receptor-deficient and apolipoprotein E-deficient mice. *J. Lipid Res.* **36,** 2320–2328 (1995).
28. Dansky, H. M., Charlton, S. A., McGee Harper, M. & Smith, J. D. T and B lymphocytes play a minor role in atherosclerotic plaque formation in the apolipoprotein E-deficient mouse. *Proc. Natl Acad. Sci. USA* **94,** 4642–4646 (1997).
29. Roselaar, S. E., Kakkanathu, P. X. & Daugherty, A. Lymphocyte populations in atherosclerotic lesions of ApoE–/– and LDL receptor–/– mice. Decreasing density with disease progression. *Arterioscler. Thromb. Vasc. Biol.* **16,** 1013–1018 (1996).

Acknowledgements. We thank E Shvartz, E. Rabkin, and E. Simon-Morrissey for technical assistance; W. C. Fanslow III for providing the rat anti-mouse-CD40L antibody; and M. W. Freeman, K. J. Moore and V. Kunjathoor for assistance and discussions. This work was supported in part by grants from the NHLBI (to P. L.) and from the Fond National Suisse pour la Recherche Scientifique (to F. M.).

Correspondence and requests for materials should be addressed to P. L. (e-mail: plibby@rics.bwh.harvard.edu).

Truncating mutations of hSNF5/INI1 in aggressive paediatric cancer

Isabella Versteege*, Nicolas Sévenet*, Julian Lange*, Marie-Françoise Rousseau-Merck*, Peter Ambros†, Rupert Handgretinger‡, Alain Aurias* & Olivier Delattre*

** Laboratoire de Pathologie Moléculaire des Cancers, Section de Recherche, Institut Curie, 26 rue d'Ulm, 75248 Paris Cedex 05, France*
† CCRI, St Anna Kinderspital, Kinderspitalgasse 6, A-1090 Vienna, Austria
‡ Universität Kinderklinik, Rümelinstrasse 23, D-72070 Tübingen, Germany

Malignant rhabdoid tumours (MRTs) are extremely aggressive cancers of early childhood. They can occur in various locations, mainly the kidney, brain and soft tissues[1,2]. Cytogenetic and molecular analyses have shown that the deletion of region 11.2 of the long arm of chromosome 22 (22q11.2) is a recurrent genetic characteristic of MRTs, indicating that this locus may encode a tumour suppressor gene[3–8]. Here we map the most frequently deleted part of chromosome 22q11.2 from a panel of 13 MRT cell lines. We observed six homozygous deletions that delineate the smallest region of overlap between the cell lines. This region is found in the *hSNF5/INI1* gene, which encodes a member of the chromatin-remodelling SWI/SNF multiprotein complexes[9–12]. We analysed the sequence of *hSNF5/INI1* and found frameshift or nonsense mutations of this gene in six other cell lines. These truncating mutations of one allele were associated with the loss of the other allele. Identical alterations were observed in corresponding primary tumour DNAs but not in matched constitutional DNAs, indicating that they had been acquired somatically. The observation of bi-allelic alterations of *hSNF5/INI1* in MRTs suggests that loss-of-function mutations of *hSNF5/INI1* contribute to oncogenesis.

To map in detail the homozygous deletions of chromosome band 22q11.2 that are observed in MRTs[7,8], we amplified 22q11.2 loci from MRT DNAs using the polymerase chain reaction (PCR). We used DNAs from established cell lines to avoid DNA contamination from non-tumour tissues. First, we tested 167 chromosome-22 loci from the DNA of a recently described MRT cell line[8]. For nine markers, specific PCR products were not detected in the tumour DNA, although the matched constitutional DNA promoted efficient amplification (cell line DL; Fig. 1). This suggested that the loci defined by these markers lay within the previously suspected homozygous deletion of 22q11.2 in DL[8]. These 9 markers and 49 flanking markers were then tested on the DNA from 12 other MRT cell lines. Loss of heterozygosity (LOH) was detected at polymorphic loci in three cases for which constitutional DNA was

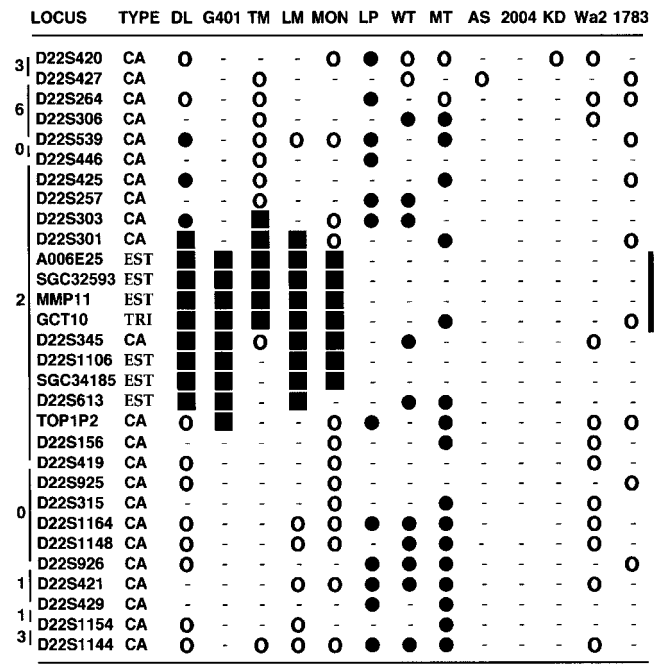

Figure 1 The commonly deleted region in MRTs contains markers A006E25, SGC32593, MMP11 and GCT10. Results of the analysis of a subset of the markers tested by PCR amplification are indicated. At the left, the distances between markers are indicated in cM (centimorgans)[29]. Filled squares indicate complete absence of amplification of a marker in the tumour DNA. Open and filled circles indicate retention and loss-of-heterozygosity of a marker sequence, respectively. A dash indicates the presence of a single PCR product in constitutional and/or tumour DNA. The type of marker is indicated: CA, dinucleotide polymorphic marker; TRI, trinucleotide polymorphic marker. The black bar at the right indicates the common region of deletion.

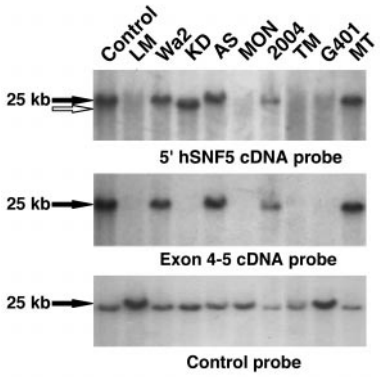

Figure 2 Homozygous deletion of exons 4 and 5 of *hSNF5/INI1* in the KD cell line. *Eco*R1-digested DNAs migrated on a 0.8% agarose gel were Southern-blotted and hybridized successively with a 5′-*hSNF5/INI1* cDNA probe (exon 1–6) (*5′-hSNF5*) and an exon 4–5 cDNA probe. Black arrows indicate the 25-kb germline DNA fragment and the white arrow shows the rearranged fragment in KD DNA. As a control for the quality of DNA in the 25-kg range, the same blot was hybridized with the SHGC-33468 EST probe.

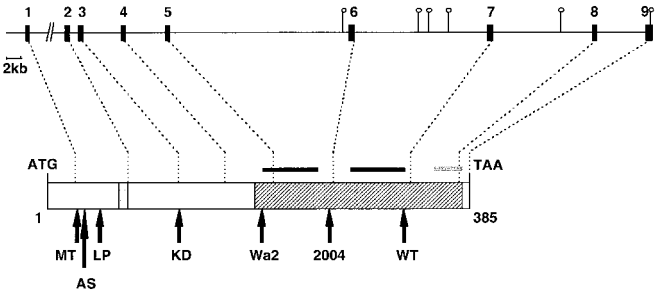

Figure 3 Genomic organization of the *hSNF5/INI1* gene and position of the stop codons generated by mutations of the coding sequence. The gene is shown at the top, and the protein at the bottom. Black boxes (top) indicate the position of exons (numbered 1–9). The localization of exons 5, 7 and 8 is not precisely known within respective *Eco*R1 sites (indicated by open circles). The hatched area represents the SNF5 domain. The grey box (bottom left) indicates a peptide sequence that can be present or absent in the protein, depending on the use of a cryptic splice donor site in exon 2. The black and grey bars above the hSNF5 protein indicate the peptide repeats of the SNF5 domain and the possible C-terminal coiled-coil structure, respectively. Arrows indicate the position of stop codons generated by point mutations in the different tumours.

available (cell lines LP, WT and MT; Fig. 1), and highly probable in four other tumour DNAs with a single allele at numerous 22q11.2 polymorphic loci (cell lines AS, 2004, KD and Wa2; Fig. 1). We observed a complete absence of amplification of several loci in four additional cell lines (G401, TM, LM and MON; Fig. 1). From these results we could delineate a common region of deletion that includes markers A006E25, SGC32593, MMP11 and GCT10.

To eliminate the possibility that we were detecting artefacts of PCR, we confirmed that these loci were homozygously deleted by Southern blotting and hybridization of MRT DNAs with ^{32}P-labelled PCR products of the markers. This showed the complete absence, as compared with control DNAs, of the expected fragments in the DNAs from DL, G401, TM, LM and MON cell lines, an observation in agreement with the PCR results (data not shown). We used these markers to screen human bacteriophage P1-based artificial chromosome (PAC) and chromosome-22-specific cosmid libraries. The analysis of overlapping clones indicated that the common region of deletion spans less than 150 kilobases (kb) of DNA (data not shown).

A006E25 is an expressed sequence tag (EST) for *hSNF5/INI1*, a human homologue of the yeast *SNF5* gene[9,10]. *hSNF5/INI1* encodes a member of the SWI/SNF complexes, which are thought to facilitate the transcriptional activation of inducible genes through the remodelling of chromatin[11–15]. We focused on this gene because hybridization of a Southern blot of MRT DNAs with a 5′-*hSNF5/INI1* probe revealed an altered migration pattern of the germline 25-kb *Eco*R1 fragment of KD DNA (Fig. 2). To study this alteration further, we determined the genomic organization of the *hSNF5/INI1* gene on cosmid DNA by direct sequencing of exon/intron boundaries with primers derived from the complementary DNA sequence. This indicated that the peptide sequence of the *hSNF5/INI1* gene is encoded by nine exons and that this gene extends over ~50 kb (Fig. 3). The amplification by reverse transcription with PCR (RT-PCR) and sequence of *hSNF5/INI1* messenger RNAs from the KD cell line showed an out-of-frame junction between exons 3 and 6. Furthermore, no PCR products were obtained for exons 4 and 5 using genomic DNA from this cell line as a template. The hybridization of the Southern blot of MRT DNAs with an *hSNF5/INI1* cDNA probe consisting of exons 4 and 5 detected the expected 25-kb fragments from control DNAs, but no signal from the KD DNA, showing that the altered migration pattern of this fragment was linked to a genomic deletion that includes these two exons (Fig. 2). These results showed that the smallest region of homozygous deletion observed in MRTs lay within the *hSNF5/INI1* gene.

We searched for mutations of the *hSNF5/INI1* gene in the seven non-homozygously deleted cell lines by direct sequencing of both RT-PCR-amplified *hSNF5/INI1* mRNAs and PCR products of individual exons obtained with primers derived from intron sequences. In six cases, DNA variants were identified (Table 1).

Table 1 Analysis of the *hSNF5/INI1* gene in cell lines, primary tumours and constitutional DNAs from MRT patients

Name of cell line	Age*	Localization	Cytogenetics	Analysis of RNA and DNA			
				Cell lines		Primary	
				Allele 1	Allele 2	tumour†	Constitutional
DL	14	Lung	46XY, t(1;22)	Deletion	Deletion	–	Two alleles
LP	12 years	Kidney	46XY	47TAC/TAA	Deletion	id	Two alleles, NS
WT	21	Kidney	46XY,-15,der15 t(1;15)	317, del 1 bp	Deletion	id	Two alleles, NS
MT	1	Soft tissue	46XY	31, ins 72 bp‡	Deletion	id	Two alleles, NS
G401	3	Kidney	46XY	Deletion	Deletion	–	–
MON	6	Abdomen	46XY,t(7;22)	Deletion	Deletion	–	Two alleles
TM	21	Retroperitoneal	46XY,t(11;22)	Deletion	Deletion	–	–
2004	6	Kidney	46XY	258, del 13 bp, ins 2 bp	Deletion	id	Two alleles, NS
1783	6	Kidney	46XY	NAD	NAD	–	–
KD	11	Abdomen	46XX, 9p+	Deletion of exons 4 and 5	Deletion	–	–
LM	8	Liver	46XX,3p+, 22q–	Deletion	Deletion	–	–
Wa2	17	Intraspinal	46XY,t(18;22)	196, dup 17 bp	Deletion	–	–
AS	7	Abdomen	46XX	37, del 19 bp	Deletion	–	–

*Age of the patient is shown in months except for the LP cell line. † Tumour material is derived from surgical biopsy. ‡ This insertion contains an in-frame stop codon. Deletion indicates a complete deletion of the *hSNF5/INI1* gene; NAD, no alteration detected; dash, no material available for analysis; id, identical alterations observed in the primary tumour and in the cell line; NS, normal sequence. For each point mutation, the position of the codon and the type of alteration are indicated; bp, base pairs; del, deletion; ins, insertion; dup, duplication.

Frameshifts due to nucleotide deletions and/or insertions were detected in five cases and a TAC-to-TAA nonsense mutation was observed in one case (Table 1). These alterations were observed in both cDNAs and corresponding genomic sequences. Double sequences, which might have been indicative of the presence of a wild-type *hSNF5/INI1* allele, were not detected. This observation confirmed LOH analyses and showed the alteration of both alleles in these six cases.

To exclude *in vitro* growth as a cause of these mutations, we analysed DNAs isolated from the matched primary tumours. Identical mutations were observed in all tested cases, establishing their presence in the original tumour cells (Table 1). Matched constitutional DNA was available in six cases. For four cases in which precise sequence alterations were found in tumour DNA (tumours LP, WT, MT and 2004), matched constitutional DNAs contained wild-type sequences. In two tumours with homozygous deletions (DL and MON), constitutional DNAs exhibited heterozygosity at the GCT10 locus (Table 1). Finally, neither LOH nor aberrant sequences could be detected in the 1783 tumour DNA. This may indicate that subtle mutations affecting non-coding sequences, including the promoter region, may have occurred in this tumour. Alternatively, it may indicate that, in rare cases of MRT, *hSNF5/INI1* may not be altered, or that, the diagnosis of MRT frequently being difficult, 1783 may be a different pathological entity to MRT.

These data show that bi-allelic, somatic alteration of *hSNF5/INI1*, arising through a combination of complete deletions of the gene, frameshift alterations and nonsense mutations, is a frequent, if not constant, feature of MRTs. This is fully consistent with the paradigm of the 'two-hit' recessive model of oncogenesis and supports the hypothesis that *hSNF5/INI1* is the MRT tumour suppressor gene. Although constitutional mutations were not detected in this study, which was based on sporadic tumours, previous reports of multifocal and/or familial MRTs indicate that constitutional inactivation of one allele of *hSNF5/INI1* could be responsible for hereditary cases[5,16]. Given the low incidence of MRTs and its aggressive evolution, which leads to frequent death at a young age, familial cases, if existing, are expected to be rare. Most of the mutations described here are predicted to truncate the phylogenetically conserved 200-amino-acid domain that mediates interactions with hbrm and with the HIV integrase[9,17]. However, the mutation in the WT cell line mainly results in the truncation of the 68 carboxy-terminal amino acids that probably form a coiled-coil structure, suggesting that the impairment of hSNF5/INI1-specific interactions, mediated by this C-terminal domain, is essential for progression of MRTs (Fig. 3).

The alteration of chromosome 22 was the only recurrent cytogenetic abnormality found in this series of tumours (Table 1)[3–8]. These observations and the high frequency of truncating mutations of *hSNF5/INI1* that we observed indicate that alteration of this gene is a major oncogenic event in MRT and could thus recapitulate several characteristics of this highly malignant paediatric cancer, including abnormal proliferation, local invasiveness and high propensity to undergo metastasis.

Accumulating evidence indicates that altered chromatin organization at specific DNA sites might be crucial in the process of oncogenesis. Indeed, the regulation of post-translational modifications of histones has been shown to be the target of alteration in cancer[18–22]. The SWI/SNF complexes, which have been identified in organisms from yeasts to humans, are also thought to be important in the remodelling of chromatin structure. Members of these complexes have also been linked to the control of cell proliferation, in particular by binding to the retinoblastoma protein[23–25]. Our results are, to our knowledge, the first to show that a member of the SWI/SNF complexes has characteristics of a tumour suppressor. The results indicate that the transcription of key genes involved in growth, differentiation or apoptotic processes could be selectively regulated by these complexes. □

Methods

Patients' samples. The TM87-16 (TM), G401, DL, 2001 and Wa2 cell lines have been described[7,8,26,27]. Other cell lines were established through *in vitro* growth of MRT cells in RPMI 1640 medium plus 10% fetal calf serum. Part of the primary tumour samples was directly frozen in liquid nitrogen. Histopathological analysis of all cases showed that the cells were round to polygonal in shape, with vesicular nuclei, prominent nucleoli, eosinophilic cytoplasm and rare but typical cytoplasmic inclusions. The cells stained positive for both keratin and vimentin and negative for desmin. Constitutional material was obtained from blood or non-tumour tissues. DNAs and RNAs were isolated using standard procedures.

PCR. The sequences of the primers were retrieved from the Genome Database (mirror site at http://gdb.infobiogen.fr/), the Whitehead Institute/MIT genome center (http://www-genome.wi.mit.edu/), the Human Gene Map (http://www.ncbi.nlm.nih.gov/SCIENCE96/), the Cooperative Human Linkage Center (http://www.chlc.org:80/), the Stanford Human Genome Center (http://www-shgc.stanford.edu) and the Sanger Center (http://www.sanger.ac.uk/). PCR was performed using the GeneAmp PCR kit (Perkin Elmer) according to the programmes provided by the above centres.

PACs and cosmid screening and sequencing. Filters from a gridded human PAC library (RPCI1,3-5 from the Lawrence Livermore National Laboratory)[28] provided by the Ressourcen Zentrum Primardaten Bank, and from a chromosome-22 library (LL22NC03), were screened with labelled PCR products from the *hSNF5/INI1* cDNA. After amplification of the positive clones, DNA was isolated using the Qiagen Plasmid kit and used to determine the *Eco*R1 restriction map of the *hSNF5/INI1* locus. Sequences of exon/intron boundaries

were obtained through direct sequencing of DNAs from overlapping cosmids with primers derived from the cDNA sequence using the AmpliTaqFS BigDye Terminator kit (Applied Biosystems). Sequencing reactions were resolved on an ABI 377 Prism automated sequencer.

Southern blot analysis. 10 μg *Eco*R1-digested cell-line and constitutional DNAs from MRT patients and from non-affected controls were subjected to electrophoresis in 0.8% agarose gel, transferred to nylon membranes (Hybond N+) and successively hybridized with ^{32}P-labelled PCR products from A006E25, MMP11 and SGC32593 DNAs, 5′-*hSNF5/INI1* cDNA (exon 1–6), 3′-*hSNF5/INI1* cDNA (exon 6–9), exons 4–5 *hSNF5/INI1* cDNA and the SHGC-33468 EST probes.

Mutation detection. We completely analysed the coding sequences of both strands of both the *hSNF5/INI1* cDNAs and the genomic DNAs from each cell line. RNAs were reverse-transcribed with oligo-dT primers and resulting cDNAs were amplified using the GeneAmp RNA PCR core kit (Perkin Elmer). In each case, two overlapping PCR products corresponding to 5′-*hSNF5/INI1* and 3′-*hSNF5/INI1* cDNA were analysed. For the analysis of genomic DNA, we designed primer couples located in introns and used these primers to PCR-amplify the nine exons of *hSNF5/INI1* individually. All PCR amplification reactions were performed using the GeneAmp RNA PCR kit (Perkin Elmer) in 1.5 mM $MgCl_2$ with the following parameters: denaturation, 94 °C for 30 s; annealing, 60 °C for 30 s; and extension, 72 °C for 30 s. PCR products were directly sequenced using the AmpliTaqFS Dye or BigDye Terminator kits (Applied Biosystems) on automatic 373A or 377 Prism sequencers. Primer sequences are available on request.

Received 26 February; accepted 7 May 1998.

1. Parham, D. M., Weeks, D. A. & Beckwith, J. B. The clinicopathologic spectrum of putative extrarenal rhabdoid tumours. An analysis of 42 cases studied with immunohistochemistry or electron microscopy. *Am. J. Surg. Pathol.* **18,** 1010–1029 (1994).
2. Wick, M. R., Ritter, J. H. & Dehner, L. P. Malignant rhabdoid tumours: a clinicopathologic review and conceptual discussion. *Semin. Diagn. Pathol.* **12,** 233–248 (1995).
3. Douglass, E. C. *et al*. Malignant rhabdoid tumour: a highly malignant childhood tumour with minimal karyotypic changes. *Gene Chromosom. Cancer* **2,** 210–216 (1990).
4. Shashi, V., Lovell, M. A., von Kap-herr, C., Waldron, P. & Golden, W. L. Malignant rhabdoid tumour of the kidney: involvement of chromosome 22. *Gene Chromosom. Cancer* **10,** 49–54 (1994).
5. Fort, D. W., Tonk, V. S., Tomlinson, G. E., Timmons, C. F. & Schneider, N. R. Rhabdoid tumour of the kidney with primitive neuroectodermal tumour of the central nervous system: associated tumours with different histologic, cytogenetic, and molecular findings. *Gene Chromosom. Cancer* **11,** 146–152 (1994).
6. Schofield, D. E., Beckwith, J. B. & Sklar, J. Loss of heterozygosity at chromosome regions 22q11-12 and 11p15.5 in renal rhabdoid tumours. *Gene Chromosom. Cancer* **15,** 10–17 (1996).
7. Biegel, J. A. *et al*. Narrowing the critical region for a rhabdoid tumour locus in 22q11. *Gene Chromosom. Cancer* **16,** 94–105 (1996).
8. Rosty, C. *et al*. Cytogenetic and molecular analysis of a t(1;22)(p36;q11.2) in a rhabdoid tumour with a putative homozygous deletion of chromosome 22. *Gene Chromosom. Cancer* **21,** 82–89 (1998).
9. Muchardt, C., Sardet, C., Bourachot, B., Onufryk, C. & Yaniv, M. A human protein with homology to *Saccharomyces cerevisiae* SNF5 interacts with the potential helicase hbrm. *Nucleic Acid. Res.* **23,** 1127–1132 (1995).
10. Kalpana, G. V., Marmon, S., Wang, W., Crabtree, G. R. & Goff, S. P. Binding and stimulation of HIV-1 integrase by a human homolog of yeast transcription factor SNF5. *Science* **266,** 2002–2006 (1994).
11. Peterson, C. L. Multiple SWItches to turn on chromatin? *Curr. Opin. Genet. Dev.* **6,** 171–175 (1996).
12. Wang, W. *et al*. Diversity and specialisation of mammalian SWI/SNF complexes. *Genes Dev.* **10,** 2117–2130 (1996).
13. Kwon, H., Imbalzano, A. N., Khavari, P. A., Kingston, R. E. & Green, M. R. Nucleosome disruption and enhancement of activator binding by a human SW1/SNF complex. *Nature* **370,** 477–485 (1994).
14. Owen-Hughes, T., Utley, R. T., Côté, J., Peterson, C. L. & Workman, J. L. Persistent site-specific remodeling of a nucleosome array by transient action of the SWI/SNF complex. *Science* **273,** 513–516 (1996).
15. Côté, J., Quinn, J., Workman, J. L. & Peterson, C. L. Stimulation of GAL4 derivative binding to nucleosomal DNA by the yeast SWI/SNF complex. *Science* **265,** 53–60 (1994).
16. Lynch, H. T. *et al*. Paravertebral malignant rhabdoid tumour in infancy. *In vitro* studies of a familial tumour. *Cancer* **52,** 290–296 (1983).
17. Morozov, A., Yung, E. & Kalpana, G. V. Structure-function analysis of integrase interactor 1/hSNF5L1 reveals differential properties of two repeat motifs present in the highly conserved region. *Proc. Natl Acad. Sci. USA* **95,** 1120–1125 (1998).
18. Sobulo, O. M. *et al*. MLL is fused to CBP, a histone acetyltransferase, in therapy-related acute myeloid leukemia with a t(11;16)(q23;p13.3). *Proc. Natl Acad. Sci. USA* **94,** 8732–8737 (1997).
19. Magnaghi-Jaulin, L. *et al*. Retinoblastoma protein represses transcription by recruiting a histone deacetylase. *Nature* **391,** 601–604 (1998).
20. Brehm, A. *et al*. Retinoblastoma protein recruits histone deacetylase to repress transcription. *Nature* **391,** 597–601 (1998).
21. Lin, R. J. *et al*. Role of histone deacetylase complex in acute promyelocytic leukaemia. *Nature* **391,** 811–814 (1998).
22. Grignani, F. Fusion proteins of the retinoic acid receptor-α recruit histone deacetylase in promyelocytic leukaemia. *Nature* **391,** 815–818 (1998).
23. Dunaief, J. L. *et al*. The retinoblastoma protein and BRG1 form a complex and cooperate to induce cell cycle arrest. *Cell* **79,** 119–130 (1994).
24. Trouche, D., Le Chalony, C., Muchardt, C., Yaniv, M. & Kouzarides, T. RB and hbrm cooperate to repress the activation functions of E2F1. *Proc. Natl Acad. Sci. USA* **94,** 11268–11273 (1997).
25. Muchardt, C., Bourachot, B., Reyes, J-C. & Yaniv, M. *ras* transformation is associated with decreased expression of the brm/SNF2α ATPase from the mammalian SWI-SNF complex. *EMBO J.* **16,** 101–109 (1998).
26. Soulié, J., Rousseau-Merck, M.-F., Mouly, H. & Nezelof, C. Cytogenetic study of cell lines from an infantile hypercalcemic renal tumour. *Cancer Genet. Cytogenet.* **21,** 117–122 (1985).
27. Handgretinger, R. *et al*. Establishment and characterisation of a cell line (Wa-2) derived from an extrarenal rhabdoid tumour. *Cancer Res.* **50,** 2177–2182 (1990).
28. Iaonnou, P. *et al*. A new bacteriophage P1-derived vector for the propagation of large human DNA fragments. *Nature Genet.* **6,** 84–89 (1994).
29. Dib, C. *et al*. A comprehensive genetic map of the human genome based on 5,264 microsatellites. *Nature* **380,** 152–154 (1996).

Acknowledgements. We thank M. Yaniv and C. Muchardt for discussions; T. Melot, A. Laugé, S. Pagès, M. Peter, I. Legrand, C. Rosty, J. Couturier and D. Stoppa-Lyonnet for their help; and the following clinicians for providing samples used in this study: F. Doz, J. Michon, H. Pacquement, E. Quintana, P. Ruck and J.-M. Zucker. I.V. and N.S. are recipients of fellowships from the European Union and the Ministère de l'Education Nationale, de la Recherche et de la Technologie, respectively. This work was supported by grants from the Association pour la Recherche contre le Cancer, the Ligue Nationale Contre le Cancer, the Institut Curie and the Programme Hospitalier de Recherche Clinique.

Correspondence and requests for materials should be addressed to O.D. (e-mail: delattre@curie.fr). EMBL accession numbers for intron–exon boundaries of *hSNFS/INI1* are Y17118–Y17126.